Molecular Biology of the Cell
Vol. 11, 1213–1224, April 2000

Axonal Membrane Proteins Are Transported in Distinct Carriers: A Two-Color Video Microscopy Study in Cultured Hippocampal Neurons[V]

Christoph Kaether,* Paul Skehel,† and Carlos G. Dotti*‡

*European Molecular Biology Laboratory, Cell Biology Program, 69012 Heidelberg, Germany; and †Division of Neurophysiology, National Institute for Medical Research, London NW7 1AA, United Kingdom

Submitted October 21, 1999; Revised January 13, 2000; Accepted February 2, 2000
Monitoring Editor: Jennifer Lippincott-Schwartz

Neurons transport newly synthesized membrane proteins along axons by microtubule-mediated fast axonal transport. Membrane proteins destined for different axonal subdomains are thought to be transported in different transport carriers. To analyze this differential transport in living neurons, we tagged the amyloid precursor protein (APP) and synaptophysin (p38) with green fluorescent protein (GFP) variants. The resulting fusion proteins, APP-yellow fluorescent protein (YFP), p38-enhanced GFP, and p38-enhanced cyan fluorescent protein, were expressed in hippocampal neurons, and the cells were imaged by video microscopy. APP-YFP was transported in elongated tubules that moved extremely fast (on average 4.5 μm/s) and over long distances. In contrast, p38-enhanced GFP-transporting structures were more vesicular and moved four times slower (0.9 μm/s) and over shorter distances only. Two-color video microscopy showed that the two proteins were sorted to different carriers that moved with different characteristics along axons of doubly transfected neurons. Antisense treatment using oligonucleotides against the kinesin heavy chain slowed down the long, continuous movement of APP-YFP tubules and increased frequency of directional changes. These results demonstrate for the first time directly the sorting and transport of two axonal membrane proteins into different carriers. Moreover, the extremely fast-moving tubules represent a previously unidentified type of axonal carrier.

INTRODUCTION

In neurons, newly synthesized proteins have to travel tremendous distances to their final destinations. For proper function and maintenance of both the elaborate dendritic tree and the sometimes extremely elongated axon, neurons need to have a fast and precise delivery system for newly synthesized proteins. In recent years, many studies have led to the identification of a variety of motor proteins and accessory molecules necessary for axonal transport. In fact, the first molecular motor protein to be identified, kinesin, was isolated from squid giant axons (Vale *et al.*, 1985a) and chick brain (Brady, 1985). Currently it is believed that there are a number of different microtubule motor proteins, kinesin superfamily proteins (KIFs), each of which is responsible for a specific set of cargo (for review, see Hirokawa, 1997; Hirokawa *et al.*, 1998). KIF1A, for example, was shown to transport vesicles containing a subset of synaptic vesicle proteins (Okada *et al.*, 1995; Yonekawa *et al.*, 1998), whereas KIF2 transported a distinct class of vesicles (Noda *et al.*, 1995).

According to this concept at least two sorting steps would be needed: different axonal membrane proteins first are segregated and packed into different carriers, presumably at the level of the *trans*-Golgi network. These carriers are then separated from those carriers destined for the somatodendritic domain and transported into the axon. Therefore, there might exist several different axonal sorting signals, for the sorting into distinct carriers and for subsequent axonal targeting. Interestingly, no conserved axonal sorting signal has been described to date (Winckler and Mellman, 1999).

The amyloid precursor protein (APP) is an ubiquitously expressed type I transmembrane protein of unknown function. A small cleavage product of APP, Aβ, is the principle

[V] Online version of this article contains video material for Figures 4, 5, 8, and 9. Online version available at www.molbiolcell.org.

‡ Corresponding author. E-mail address: dotti@embl-heidelberg.de.

Abbreviations used: APP, amyloid precursor protein; ECFP, enhanced cyan fluorescent protein; EGFP, enhanced GFP; FP, fluorescent protein; GFP, green fluorescent protein; KHC, kinesin heavy chain; KIF, kinesin superfamily protein; p38, synaptophysin; Rh-dextran, rhodamine-dextran; YFP, yellow fluorescent protein.

© 2000 by The American Society for Cell Biology

constituent of the amyloid plaques in the brains of Alzheimer's disease patients (for review, see Selkoe, 1999). In neurons, newly synthesized APP is targeted to the axon and subsequently transcytosed to the somatodendritic domain (Simons *et al.*, 1995; Yamazaki *et al.*, 1995). Radioactive labeling studies suggested that APP is transported into the axon by fast axonal transport (Koo *et al.*, 1990) dependent on conventional kinesin (Amaratunga *et al.*, 1993; Ferreira *et al.*, 1993; Buxbaum *et al.*, 1998). In the amyloidogenic pathway, APP cleavage leads to the production of Aβ, or, more abundantly, cleavage in the nonamyloidogenic pathway leads to a soluble APP and a membrane-bound C-terminal fragment. Cleavage in the amyloidogenic pathway is mediated by β- and γ-secretase and in the nonamyloidogenic pathway by α-secretase (summarized by Hardy, 1997; Selkoe, 1999). Despite numerous efforts, the molecular identities of the secretases have not yet been fully established. For a better understanding of the mechanisms that govern APP processing in neurons, it appears essential to precisely characterize the subcellular localization of APP at any given stage of its short lifetime, calculated to be 20–30 min, in PC12 cells and neurons (Weidemann *et al.*, 1989; Storey *et al.*, 1999).

We therefore decided to follow the fate of newly synthesized APP directly in living cultured hippocampal neurons and to characterize its mode of transport. Hippocampal neurons have been used extensively as a model system of transport and protein sorting (Craig and Banker, 1994). Moreover, the hippocampus is one of the predominantly affected regions in Alzheimer's disease (Selkoe, 1999). Therefore, hippocampal neuronal cultures are a particularly useful and relevant system with which to study APP trafficking and transport.

In the present study we expressed a fluorescent protein (FP)-tagged APP in hippocampal neurons and analyzed its transport by video microscopy. FP-tagged APP moves along axons in very fast-moving elongated tubules, which have not been described previously. We show by two-color video microscopy that these tubules are different from the transport carriers of another axonal membrane protein, synaptophysin (p38).

MATERIALS AND METHODS

Antibodies

For detection of APP we used monoclonal antibody 22C11 (Roche Diagnostics, Mannheim, Germany); for detection of green fluorescent protein (GFP) we used a polyclonal antibody from Clontech Laboratories (Palo Alto, CA) and a polyclonal antibody raised against the C terminus (D2; Wacker *et al.*, 1997), kindly provided by Dr. H.-H. Gerdes (Department of Neurobiology, University Heidelberg, Heidelberg, Germany). To stain dendrites we used a monoclonal anti-MAP2 antibody (Sigma, Deisenhofen, Germany).

Construction of Fusion Proteins

APP-Yellow Fluorescent Protein (YFP). Standard molecular cloning techniques were used throughout. YFP5 cDNA (Pepperkok *et al.*, 1999) without the start codon was fused to the 3′end of human APP695 cDNA omitting the stop codon. The introduction of the restriction site, *Not*I, resulted in a linker sequence coding for three alanines. YFP5 was amplified with PCR using primer 5′-GCGCGCGGCCGCGGGTAAAGGAGAAGAACTTTTC, introducing a *Not*I site (underlined), and primer 5′-GCGCGGGCCCTAGAAGCTTTTGTATAGTTC, introducing *Apa*I. The obtained fragment was subcloned using the TOPO-TA cloning kit (Invitrogen, Groningen, The Netherlands), and the resulting plasmid, pCR-TOPO/YFP, was digested with *Not*I and *Apa*I. The YFP fragment was purified and then subcloned in pcDNA3 (Invitrogen), yielding pcDNA3/YFP. APP was amplified from pSG5-hAPP695 (kindly provided by B. de Strooper, Center for Human Genetics, Leuven, Belgium) using primer 5′-GCGCGATATCGCCACCATGCTGCCCGGTTTGGCACTGCTC, introducing *Eco*RV (underlined) and a Kosak sequence (dashed line), and primer 5′-GCGCGCGGCCGCGTTCTGCATCTGCTCAAAGAACTTG, introducing *Not*I (underlined). The fragment was cloned in pCR-TOPO, digested with *Eco*RV and *Not*I, and subcloned in pcDNA3/YFP to obtain pcDNA3/APP-YFP. Relevant parts including the Aβ-domain, the transmembrane and cytoplasmic domains of APP, as well as the transition site of the construct were sequenced.

p38-Enhanced GFP (EGFP) and p38-Enhanced Cyan Fluorescent Protein (ECFP). A plasmid encoding for a GFP-tagged p38 was constructed by amplifying rat p38 cDNA (Leube *et al.*, 1987) using primer 5′-CTGCAAGCTTCGGACATGGACGTGGTG, introducing *Hin*dIII (underlined) and primer 5′-GACCGTCGACCATCTGATTGGAGAAGG, introducing *Sal*I (underlined) and replacing the stop codon with a valine codon. The purified fragment was *Hin*dIII and *Sal*I digested and cloned in pEGFP-N3 (Clontech). The construct was sequenced, and a point mutation was found, changing codon 185 from C to R, apparently without observable effects, because a construct with a reversed mutation behaved very similar (our unpublished results). Moreover, the dynamics are very similar to another p38-GFP construct (Nakata *et al.*, 1998).

For p38-ECFP the p38 cDNA was amplified from p38-EGFP using the primer 5′-AAGCTTGCCACCATGGACGTGGTGAATCAG, covering the *Hin*dIII site (underlined), and the primer 5′-GTCGACCACCATCTGATTGGAGAAGGAG, using the *Sal*I site (underlined). After subcloning in pCR-TOPO, digestion with *Hin*dIII–*Sal*I, and gel purification, the fragment was subcloned in pECFP-N1 (Clontech).

Cell Culture and Transient Transfection

Cultures of embryonic day 18 rat embryonic hippocampal neurons were prepared as described (de Hoop *et al.*, 1998). Neurons were transfected at days 6–8 in vitro, corresponding to stage 4 neurons (Dotti *et al.*, 1988). For transfection, a calcium phosphate precipitation protocol was used (Köhrmann *et al.*, 1999). Neurons grown on 15-mm coverslips were transferred to 3.5-cm dishes containing 2 ml of conditioned medium. Alternatively, the medium of neurons grown on poly-L-lysine–coated 3.5-cm dishes was replaced with conditioned medium. Two to 3 μg of endotoxin-free (EndoFree Maxi Prep; Qiagen, Hilden, Germany) plasmid DNA were dissolved in 60 μl of 250 mM $CaCl_2$. A 2× concentration of BBS (280 mM NaCl, 1.5 mM Na_2HPO_4, and 50 mM *N,N*-bis[2-hydroxyethyl]-2-aminoethanesulfonic acid, pH 7.05) was added slowly, and the precipitate was allowed to form for 1 min. This solution was added to the cells, and the dishes were incubated for 1–2 h at 37°C and 2.5% CO_2. Cells were then washed twice in HBS (135 mM NaCl, 20 mM HEPES, 4 mM KCl, 1 mM Na_2HPO_4, 2 mM $CaCl_2$, 1 mM MgCl, and 10 mM glucose, pH 7.05) before the original growth medium was added. Double transfections were done by preparing the transfection mix with the two plasmids, each at the concentration used for single transfections. Analysis of transfected cells was performed 24–28 h after the transfection. Typically 1–20% of neurons were transfected. Some neurons expressed very high amounts of exogenous proteins resulting in uniform green fluorescence. For microscopy only neurons that showed punctate fluorescence and no beading along neurites were chosen.

Immunodetection

Immunofluorescence was performed as described (Wacker *et al.*, 1997). We found that APP-YFP fluorescence was not preserved after fixation in 4% paraformaldehyde. For immunoblotting, neurons were grown on 3.5-cm dishes covered with a sterile coverslip. After transfection, 2 mM sodium butyrate was added to the medium (Stowell and Craig, 1999). Sixteen to 20 h after transfection, media of three dishes were pooled, and proteins were precipitated by adding 4 vol of acetone in the presence of BSA as a carrier. After 2 h at −20°C, samples were centrifuged, and the pellet was air dried and dissolved in running buffer. Corresponding cells were lysed in 0.1% SDS and methanol-chloroform extracted (Wessel and Flügge, 1984). Lysates and media were run on a 10% minigel (Bio-Rad, Hercules, CA) and blotted onto nitrocellulose. Western blotting was performed as described previously (Wacker *et al.*, 1997).

Rhodamine-Dextran Uptake

Endocytic organelles were labeled by incubation of neurons for 1–2 h in conditioned medium supplemented with 1 mg/ml rhodamine-dextran (Rh-dextran), molecular weight 70,000 (Sigma). Before microscopy, cells were washed in HBS and conditioned medium.

Antisense Treatment

Antisense experiments were done as previously described by Ferreira *et al.* (1992). Oligonucleotides used were GCCGGGTCCGCCATCTTTCTGGCAG, the inverse complement of the rat nucleotides −11 to + 14 of conventional kinesin heavy chain (KHC), and CTGCCAGAAAGATGGCGGACCCGGC, the corresponding sense oligonucleotide (Ferreira *et al.*, 1992). Five to 6 h later transfection oligos were added at a concentration of 0.5 μM. Twelve hours later oligos were added at a concentration of 0.25 μM. Video microscopy was performed 26–28 h after transfection. Treating cells with oligos at 50 μM (Ferreira *et al.*, 1992) led to similar results, except that even more structures changed direction of movement (our unpublished results).

Microscopy

Fixed cells were analyzed on a Zeiss (Thornwood, NY) Axiovert microscope equipped with a 40 or 63× objective using standard FITC and rhodamine filters. Images were collected with a Cohu (San Diego, CA) camera controlled by NIH Image software, combined, and processed using Photoshop (Adobe Systems, Mountain View, CA). Staining in neurites was selectively enhanced over cell bodies.

For live cell imaging of transfected neurons, coverslips were transferred to aluminum slides (Bradke and Dotti, 1997). Two video microscopy setups were used. Initial experiments and antisense experiments were performed on a Zeiss Axiovert microscope with an 37°C-heated, 63×, numerical aperture 1.4 objective, a standard FITC filter (BP485, FT510, LP520; Zeiss), a Blitz Optilas (Puchheim, Germany) shutter, a Cohu camera, and NIH image software (Bradke and Dotti, 1997). Time-lapse series for velocity determination as well as analysis of double transfected neurons were done on a Leica (Nussloch, Germany) DM IRBE equipped with a custom-made Plexiglas box for air heating to 37°C, a 63× objective, a Hamamatsu C 4742 camera (Hamamatsu Photonics, Herrsching, Germany), and OpenLab software (Improvision, Boston, MA; Toomre *et al.*, 1999). To image YFP and CFP separately, appropriate filter blocks were used (AHF Analysentechnik, Tübingen, Germany). Excitation light was attenuated with gray filters. Typically, time-lapse series were taken without delay at exposure times between 300 and 800 ms per frame. Tubular appearance attributable to movement during exposure time could account only for a maximal length of 5 μm (calculated for 1-s exposure time; average velocity, 5 μm/s), not for the 10-μm tubules observed frequently with exposure times down to 300 ms. For dual-color imaging the following setups were used. YFP and CFP were excited separately with filters (AHF) on a filter wheel.

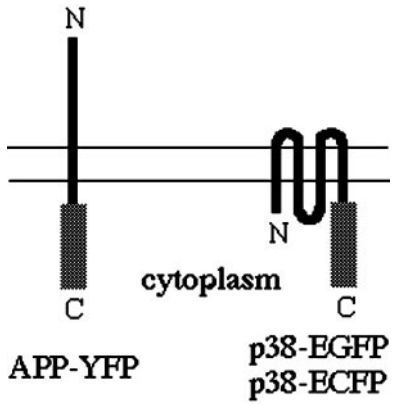

Figure 1. Schematic diagram of GFP fusion proteins.YFP was fused to the C terminus of human APP695 (left). EGFP and ECFP were fused to the C terminus of rat p38 (right). In both constructs the FP is in the cytoplasm. The double line represents the plasma membrane.

For emission, a custom-made dual beam splitter was used (AHF, blocking at 390/22, 436/10, and 515/10–15 nm). Exposure time for CFP was 110 ms and for YFP was 1 s. GFP and Rh-dextran were excited with filters for FITC and TRITC, respectively, and the emission was recorded using a dual beam splitter for FITC and TRITC. Exposure times were 1 s for GFP and 700 ms for Rh-dextran. Twenty pairs of images were recorded in 60 s. Neurons were very sensitive to CFP excitation; therefore, only series of up to 20 images could be recorded before movement of all organelles stopped.

Tracking

For particle tracking an NIH Image-based manual macro written by J. Rietdorf (European Molecular Biology Laboratory) was used. Stacks of time-lapse sequences were analyzed for movement of fluorescent structures. Only structures moving over more than three frames were evaluated. The pixel size was determined using a stage micrometer (Graticules, Tonbridge, United Kingdom), and the actual time the system needed for recording of a time-lapse series was measured. This allowed the time between subsequent frames and the distance that a tracked structure moved to be calculated. From the data, the maximal and average velocity and the displacement of fluorescent structures were calculated.

RESULTS

Construction of GFP Fusion Proteins

The aim of our study was to analyze the trafficking of APP in living neurons and compare it with the trafficking of another axonal membrane protein, the synaptic vesicle protein p38. Therefore, we tagged the human APP695 at the C terminus with a spectral variant of GFP, YFP5 (Pepperkok *et al.*, 1999). Two other fusion proteins, consisting of p38 and EGFP (p38-EGFP) and p38 and another spectral GFP variant, ECFP (p38-ECFP), were constructed. The YFP/CFP mutants were chosen to allow simultaneous visualization of two different proteins in a single cell (Ellenberg *et al.*, 1999). The fusion proteins are schematized in Figure 1.

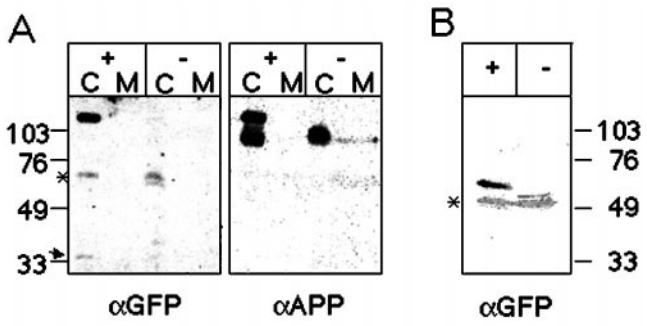

Figure 2. Transfected GFP fusion proteins are expressed as full-length proteins. (A) Cell lysates (C) and media (M) of 8-d-old APP-YFP–transfected (+) and mock-transfected (−) neurons were analyzed by SDS-PAGE and immunoblotting with GFP antiserum (αGFP). The asterisk marks a nonspecific band visible in transfected and control neurons; the arrow points to a minor degradation band. After stripping, the blot was reprobed with an antibody against APP (αAPP). Full-length APP-YFP as well as endogenous rat APP were detected. Molecular mass markers are indicated in kilodaltons (B) Cell lysates of 9-d-old p38-EGFP–transfected (+) and mock-transfected (−) neurons were analyzed by SDS-PAGE and immunoblotting with GFP antiserum D2 (αGFP). The asterisk marks a prominent nonspecific band. Molecular mass markers are indicated in kilodaltons.

FP-tagged Fusion Proteins Are Expressed as Full-Length Proteins and Sorted to Axons in Hippocampal Neurons

Before analyzing the transport of the fusion proteins by video microscopy, we ensured that the proteins were expressed as full-length proteins and that they were correctly localized. This was especially important in the case of APP-YFP, because the APP is subject to a variety of potential proteolytic cleavages. For example, extensive intracellular α- or β-secretase cleavage would generate an FP-tagged cytoplasmic tail and transmembrane domain of APP indistinguishable from intact protein by fluorescent microscopy. To check for full-length expression, hippocampal neurons were transfected with APP-YFP cDNA and analyzed by Western blot. Using a GFP-specific antibody, a prominent band with the size of the fusion protein (130 kDa) was detected in cell lysates of transfected cells (Figure 2A, left). As expected for a transmembrane protein, no signal was detected in the medium. Only a minor degradation product is visible in the cell lysate of transfected neurons (Figure 2A, arrow). To substantiate this finding, the blot was stripped and reprobed with an APP-specific antibody (Figure 2A, right). The antibody detected full-length APP-YFP as well as endogenous rat APP. If a significant amount of APP-YFP would be cleaved by α-secretase, one would expect more of the soluble APP fragment in the medium of transfected cells compared with control cells. This is not the case (Figure 2A, right). Similarly, cell lysates of neurons transfected with p38-EGFP cDNA show only the full-length fusion protein when probed with an antibody against GFP (Figure 2B). The minor lower band reflects unspecific cross-reaction of the antibody (Figure 2B, asterisk).

Because we wanted to study axonal transport, we next analyzed whether the fusion proteins would be sorted to axons after transient transfection. Therefore, neurons cultured for 6–9 d were transfected with APP-YFP and p38-EGFP cDNA, respectively, and subjected to immunofluorescence using antibodies against GFP and MAP2, a marker for dendrites. Microscopic analysis of both constructs showed that they were sorted to axons as expected (Figure 3). In addition, a somatodendritic staining was observed for both constructs. This has been found for a variety of exogenously expressed axonal and apical proteins and could be due to saturation of the axonal sorting machinery (reviewed by Winckler and Mellman, 1999). In the case of APP-YFP a somatodendritic localization of at least some of the protein could be due to transcytosis from the axon (Simons *et al.*, 1995; Yamazaki *et al.*, 1995).

Taken together, these data suggest that APP-YFP and p38-EGFP are useful markers to study axonal transport in living hippocampal neurons.

APP-YFP Is Transported along Axons in Elongated, Fast-moving Tubules

To visualize the transport of APP-YFP in the axons of living hippocampal neurons, we transfected cells with APP-YFP cDNA and analyzed the transport at 37°C by video microscopy. Typically, 24 h after transfection, expression of exogenous proteins could be observed in 1–20% of neurons. Transfected cells that appeared healthy by phase-contrast and GFP fluorescence were imaged by video microscopy. Figure 4 (video) shows six consecutive frames (0.9 s apart) of a time-lapse sequence collected from axons of transfected neurons. Long tubular structures were moving along the axons, mainly anterogradely (Figure 4, arrows) but occasionally retrogradely (Figure 4, arrowheads). In addition to the moving tubules, stationary or slow moving vesicles were present (Figure 4, asterisk). The tubular appearance of the transport carriers was not due to an artifact created by the movement of a structure during exposure time (see MATERIALS AND METHODS) or due to overexpression, because tubules were observed also in neurons expressing very low amounts of APP-YFP. The tubules were of variable length and could be as long as 10 μm. The length of a tubule was not correlated to its speed. Occasionally a tubule could be seen to stop, without losing the tubular appearance, then eventually shrinking to a vesicle before elongating again and resuming movement (our unpublished results). The tubules are not mitochondria, which also show a tubular appearance in axons (Morris and Hollenbeck, 1995), as shown by staining with rhodamine 123 (our unpublished results). Only in very few cases did the APP-YFP tubules change direction; in many cases they transversed the field of view without stopping.

To quantitate these movements, axonal transport in a number of transfected neurons was recorded. Evaluation of 8 cells from three different experiments showed that of 156 clearly discernible structures 32% (50 particles, all vesicular) did not move or only moved over a short distance (<3 μm). Forty-eight percent (75) moved anterogradely over long distances, 97.3% (73) of which were long tubules and 2.7% (2) of which were vesicular. The remaining 20% (31) were moving retrogradely, 71% (22) of which were tubular, the others vesicular.

We next tracked all structures moving >3 μm and calculated their velocity. APP-YFP–containing transport carriers

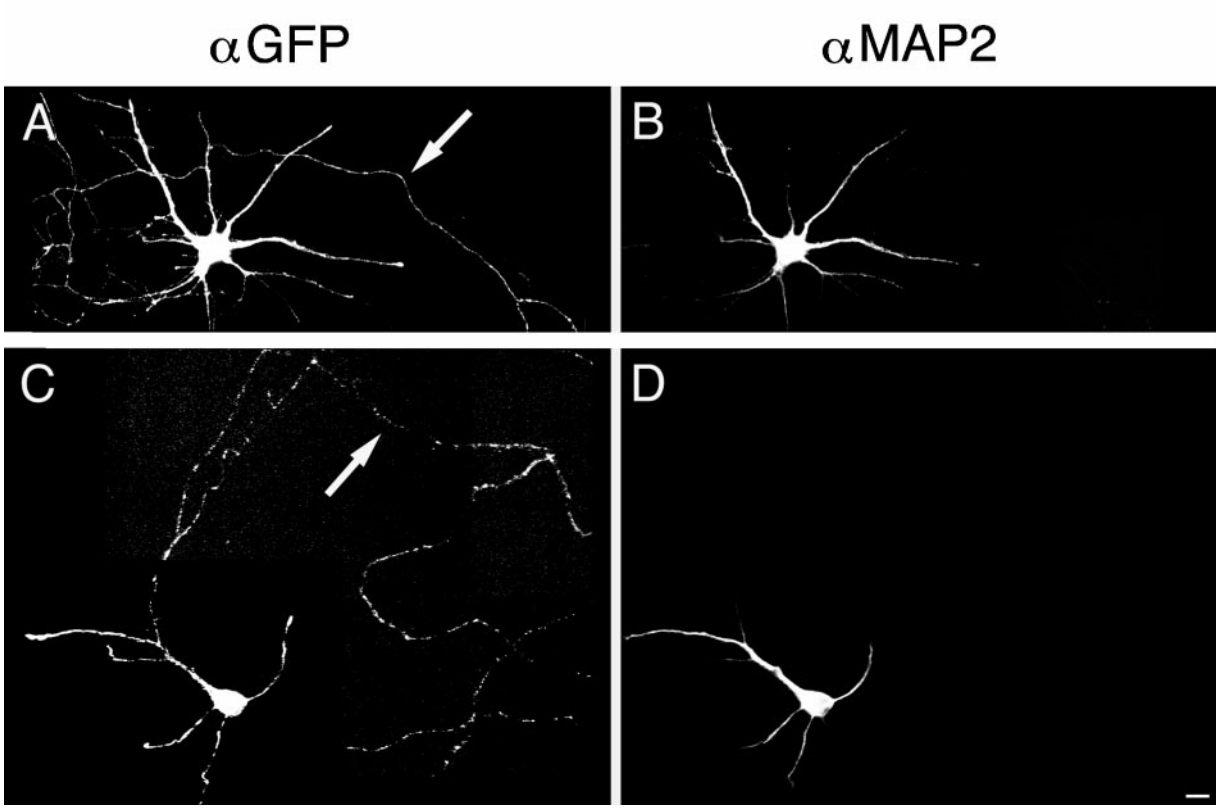

Figure 3. GFP-labeled fusion proteins are sorted to axons. Seven- to 10-d-old neurons were transfected with APP-YFP (A and B) or p38-EGFP (C and D) cDNA, fixed after 1 d, and processed for immunofluorescence using anti-GFP antiserum (αGFP) and anti-MAP2 monoclonal antibody (αMAP2). Arrows indicate axons as defined by the absence of MAP2 labeling. Bar, 10 μm.

were moving anterogradely at an average velocity of 4.5 ± 1.5 μm/s with maximal velocities of up to 9 μm/s. Retrogradely APP-YFP–containing structures moved slower, on average 2.9 ± 1 μm/s. Transport carriers could be followed on average for 53 μm before leaving the field of view or plane of focus or, rarely observed, stopping.

p38-EGFP Is Transported in Different Carriers

Are other axonal membrane proteins also transported in elongated tubules? To test this, neurons were transfected with p38-EGFP cDNA and analyzed by video microscopy (Figure 5, video). Fluorescent vesicles could be observed along the axons of transfected cells. They showed two types of movement: bright fluorescent vesicles without movement or moving over short distances (Figure 5, arrowheads) and tubulovesicular structures, often less bright, moving either anterogradely or retrogradely (Figure 5, arrows). The overall appearance, however, was strikingly different compared with the movement of APP-YFP carriers. No tubules or only short ones could be observed, and carriers rarely moved over long distances (Figure 5). The dynamics of p38-EGFP–labeled organelles are reminiscent of those of recycling endosomes recently described by Prekeris *et al.*, (1999). We therefore tested to what extent the p38-EGFP–containing organelles could be labeled with an endosomal marker. To this end, we labeled p38-EGFP–transfected neurons with Rh-dextran and analyzed them by two-color video microscopy (Figure 6). Moving p38-EGFP–labeled tubulovesicular structures were not costained with the endosomal marker, suggesting that they are transport vesicles rather than endosomes (Figure 6, arrowheads). Moving Rh-dextran–labeled organelles were often devoid of p38-EGFP staining (Figure 6, arrows). However, we sometimes observed moving structures containing both p38-EGFP and Rh-dextran (our unpublished results). In addition to the moving organelles, many immobile short tubulovesicular organelles containing both markers were observed (Figure 6, asterisks). Taken together, these data suggest that the organelles labeled by p38-EGFP are a mixture of endocytic and exocytic vesicles.

To quantify the movement of p38-EGFP fluorescent transport carriers, time-lapse microscopy of transfected neurons was analyzed as for APP-YFP. From eight cells from three independent experiments, 165 clearly discernable fluorescent carriers were tracked. Fifty-six percent (92) of p38-EGFP–containing carriers were not moving or showed brownian motion. These most likely corresponded to organelles of endocytic origin. Forty-four percent (73) showed movement over >3 μm, without directional bias. The average velocity of anterogradely moving carriers was 0.9 ± 0.9 μm/s, more than four times slower than APP-YFP–containing carriers. Retrogradely moving

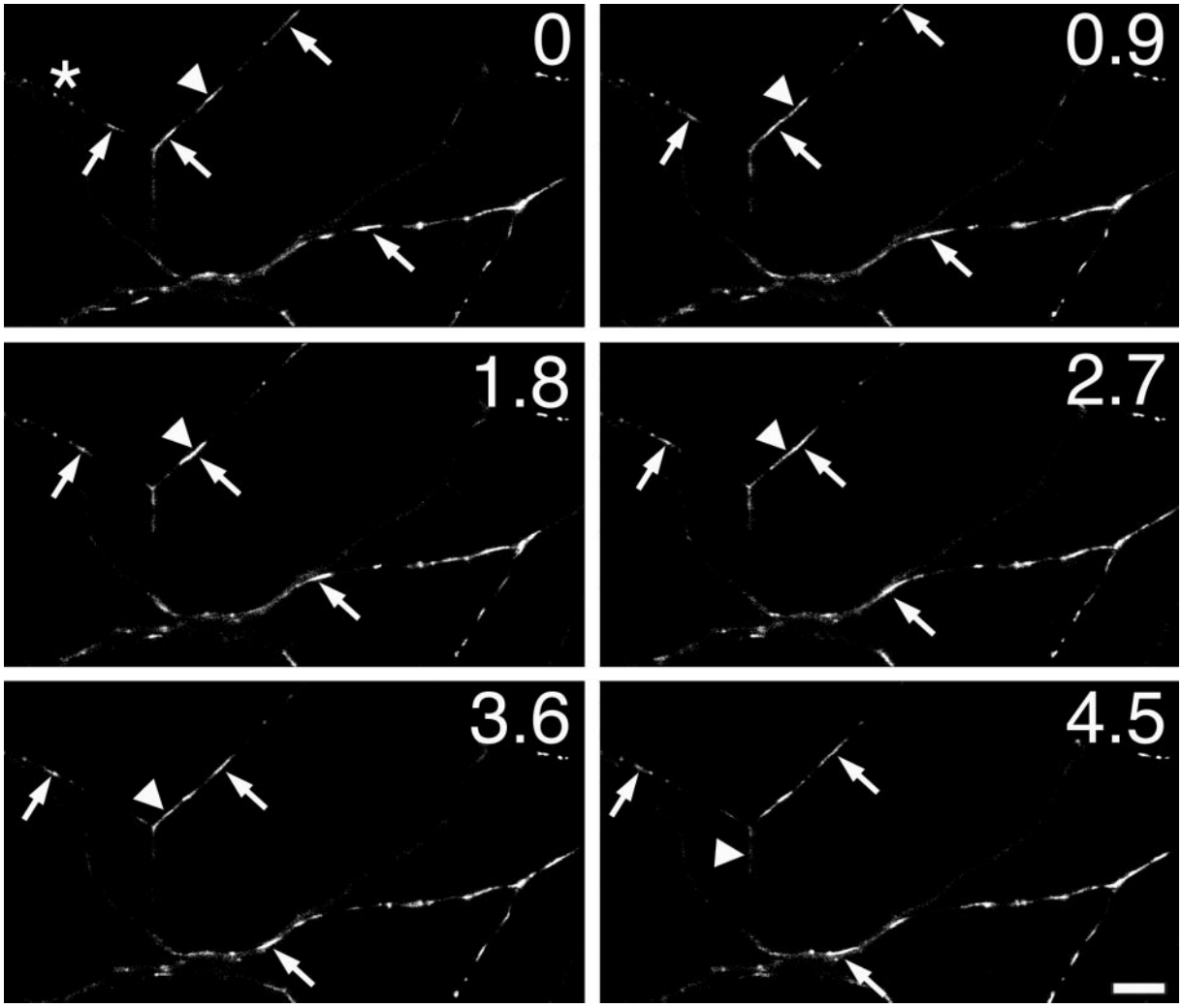

Figure 4. APP-YFP is transported in long tubules along axons (video). Nine-day-old neurons were transfected with APP-YFP cDNA and analyzed 24 h later by video microscopy. Frames were taken every 0.9 s; 6 subsequent frames of 50 frames (total length, 45 s) are shown. Arrows depict fast anterogradely moving, APP-YFP–containing tubules; arrowheads indicate retrogradely moving tubules. The asterisk points to nonmoving, vesicular structures. Bar. 10 μm.

carriers were slightly faster, on average 1.2 $\pm$ 1.2 μm/s. p38-EGFP moving structures could be tracked on average only 6.6 μm, eight times shorter than APP-YFP–containing tubules. A comparable p38-GFP has been shown to move in a similar manner in dorsal root ganglion neurons (Nakata *et al.*, 1998). Because all p38-EGFP–labeled organelles, endosomes and transport vesicles, move with dynamics strikingly different from those labeled with APP-YFP, these data suggest that the two proteins are transported in different carriers. A velocity profile of APP-YFP– and p38-EGFP–containing carriers is shown in Figure 7, and the findings are summarized in Table 1.

In Doubly Transfected Neurons, APP-YFP and p38-ECFP Are Transported in Different Carriers

APP-YFP and p38-EGFP transport carriers move in a strikingly different manner along axons, suggesting that they are sorted to different transport carriers. To directly analyze the sorting and differential transport of the two proteins in single axons, we cotransfected neurons with both APP-YFP and p38-ECFP cDNAs. Most transfected cells expressed both exogenous proteins, however, often in differing amounts. Neurons expressing approximately similar amounts of both proteins were chosen and analyzed by two-color video microscopy (Figure 8). When frames of either the YFP or CFP channel were displayed separately, they looked identical to the single transfected neurons: APP-YFP moving in long tubules (Figure 8A, left, video), p38-ECFP moving slower and in vesicular structures (Figure 8A, middle, video). Display of the merged frames shows the different movement of the two proteins along the same axon (Figure 8A, right, video). The long tubules transporting APP-YFP did not contain p38-ECFP (Figure 8B, arrows). Conversely, moving p38-ECFP–containing structures did not appear to have APP-

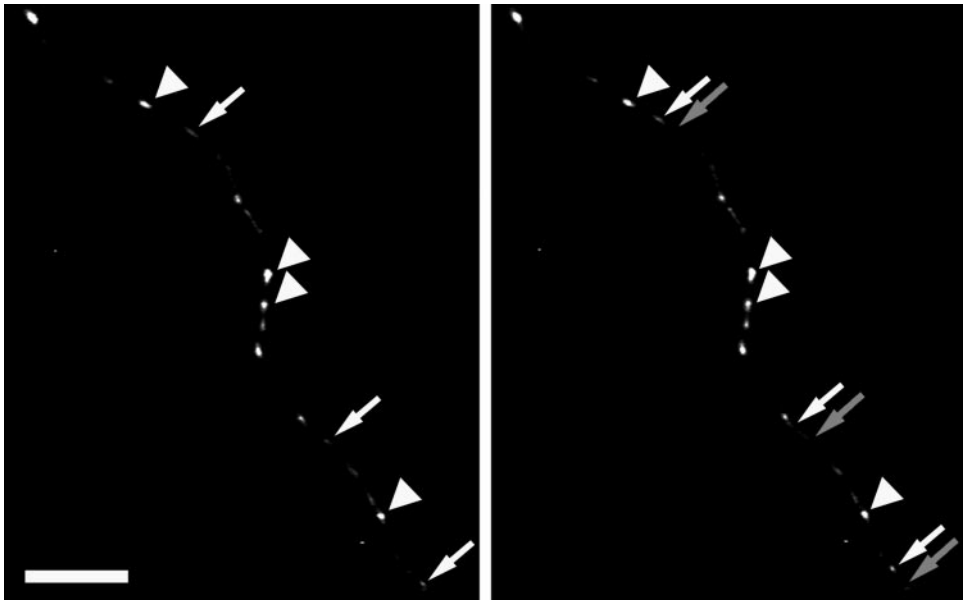

Figure 5. p38-EGFP is transported in tubulovesicular structures (video). Seven- to 8-d-old neurons were transfected with p38-EGFP cDNA and analyzed 24 h later by video microscopy. Frames were taken every 3 s; two subsequent frames of 70 (total length, 210 s) are shown. White arrows depict moving, p38-EGFP–containing tubules; gray arrows indicate the positions of the structures in the previous frame. Arrowheads point to nonmoving structures. Top, anterograde. Bar, 10 μm.

YFP (Figure 8B, triangle). Occasionally, slow or nonmoving structures containing both proteins were seen, which are possibly endosomes or multivesicular bodies (Figure 8B, arrowheads), because slow-moving, nontubular APP-YFP carriers can be labeled with Rh-transferrin (our unpublished results).

Taken together these data suggest that FP-tagged APP and p38 are sorted to and transported in carriers that differ in their morphology, their velocity, and their displacement. This implies that these carriers have a different molecular composition and are transported by the action of different motor proteins.

APP-YFP Transport Is Kinesin Dependent

Treatment of hippocampal neurons with antisense oligonucleotides against KHC and subsequent immunofluorescence suggested a role for kinesin in the fast axonal transport of APP (Ferreira *et al.*, 1993; Yamazaki *et al.*, 1995). To test the effect of kinesin on the transport of the APP-YFP tubules described here, we treated transfected neurons with KHC antisense or sense oligonucleotides. The transport of APP-YFP was then analyzed by video microscopy (Figure 9, video). In transfected neurons treated with sense oligonucleotides, the previously observed pattern of movement was observed: tubules moving over long distances and almost never changing their direction during recording of 30–70 frames (Figure 9, left, the track display of one structure is shown). In contrast, APP-YFP tubules showed a different type of movement when neurons were treated with antisense oligonucleotides: The shape of the tubules was unchanged, but their velocity was reduced. In addition, many of the observed moving structures changed their direction of

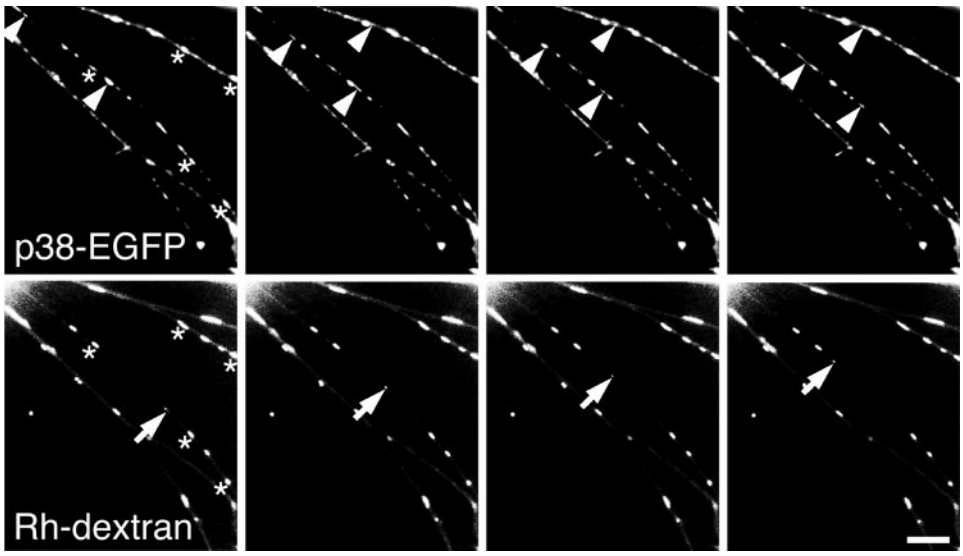

Figure 6. Moving p38-EGFP–containing vesicles do not contain an endosomal marker. Eight-day-old neurons were transfected with p38-EGFP cDNA, labeled 22 h later for 1–2 h with 1 mg/ml Rh-dextran, and analyzed by two-color video microscopy as described in MATERIALS AND METHODS. Top, consecutive frames showing p38-EGFP-fluorescence; bottom, corresponding frames showing Rh-dextran fluorescence. Arrowheads point to moving p38-EGFP–containing vesicles; arrows point to a moving Rh-dextran–containing vesicle. Asterisks mark nonmoving structures that contain both markes. Note that moving vesicles contain one marker only. Bar, 10 μm.

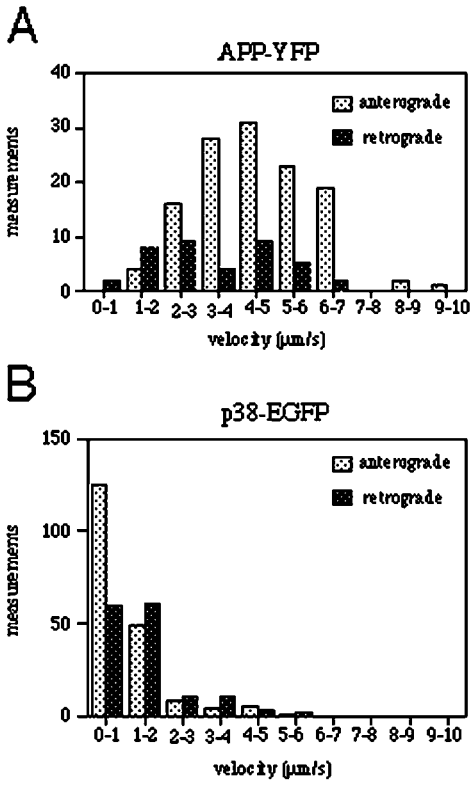

Figure 7. Velocity profile of axonal transport of APP-YFP in comparison with p38-EGFP. Neurons were transfected with APP-YFP and p38-EGFP cDNA, respectively, and analyzed by video microscopy. Moving structures were tracked, and the velocity was calculated as described in MATERIALS AND METHODS. (A) Velocity profile of APP-YFP–containing moving structures. (B) Velocity profile of p38-EGFP–containing moving structures. Measurements, number of measured velocities between two frames.

movement several times (exemplified in Figure 9, right, where the tubule changed direction four times). Quantitation of 28 cells from four experiments showed that the velocity of APP-YFP tubules in antisense-treated neurons was on average reduced to 60% of the control velocity, and that 19 of 66 (29%) of the observed tubules changed their direction at least once, compared with 3% in control neurons. Interestingly, both anterograde and retrograde transport were affected, similar to observations in squid axons (Brady *et al*., 1990). These data demonstrate that the transport of APP-YFP tubules is microtubule and kinesin dependent.

DISCUSSION

In this study we show that a fluorescently tagged APP, APP-YFP, is transported in extended, very fast-moving tubules along axons of cultured hippocampal neurons. In contrast, another axonal protein, p38, is sorted to and transported in different structures when expressed as an FP-tagged fusion protein. The two transport carriers were shown to be different by video microscopy and object tracking. Major differences were 1) morphology; whereas APP-YFP was transported in fast-moving tubules of up to 10 μm length, p38-EGFP was transported in tubulovesicular carriers; 2) velocity; APP-YFP tubules moved on average 4.5 μm/s, more than fourfold faster than structures containing p38-EGFP; and 3) mutual exclusion; fast-moving APP-YFP tubules contained no p38-ECFP when coexpressed in the same neuron and analyzed by two-color video microscopy.

The elongated, fast-moving tubules represent a previously undescribed type of transport carrier for membrane proteins. Shorter and slower moving tubulovesicular post-Golgi structures have been described in neurons (Nakata *et al*., 1998) and unpolarized cells (Hirschberg *et al*., 1998; Toomre *et al*., 1999). Axonal transport in different systems was reported to be between 1 and 3 μm/s on average, sometimes with maximal velocities of up to 5 μm/s (Allen *et al*., 1982; Kreis *et al*., 1989; Bloom *et al*., 1993; Lochner *et al*., 1998; Nakata *et al*., 1998; Zakharenko and Popov, 1998; Bridgman, 1999). The velocity measured for APP-YFP in our system is in the range of the fast component of fast axonal transport in mammals in vivo, which has been calculated to have a velocity of 410 mm/d (Ochs, 1972), corresponding to 4.7 μm/s.

The concept of separate transport carriers for subclasses of axonal membrane proteins has been proposed by Hirokawa *et al*. (1998). We confirm this concept by comparing the transport characteristics of two axonal membrane proteins and the direct observation of their differential transport in a single hippocampal neuron. To our knowledge this is the first report in which this sorting and transport of two axonal

Table 1. Characteristics of FP-tagged APP and p38

	APP-YFP	p38-EGFP (this study)	p38 GFP (Nakata *et al*., 1998)
Morphology	Mainly tubular	Mainly vesicular	Tubulovesicular
Direction	Mainly anterograde	Anterograde and retrograde	Anterograde and retrograde
Average velocity (μm/s)	4.5 ± 1.5 (anterograde) 2.9 ± 1 (retrograde)	0.9 ± 0.9 (anterograde) 1.2 ± 1.2 (retrograde)	0.69 ± 0.33
Maximal velocity (μm/s)	8–9	5	ND
Displacement (μm)	53.7 (n = 32)	6.6 (n = 34)	ND

Average velocities were determined of all measurements; the displacement is the average distance a moving structure could be tracked until it left the field of view, stopped moving, or became indistinguishable from other fluorescent structures. ND, not determined. Data on p38-GFP were taken from Nakata *et al.* (1998).

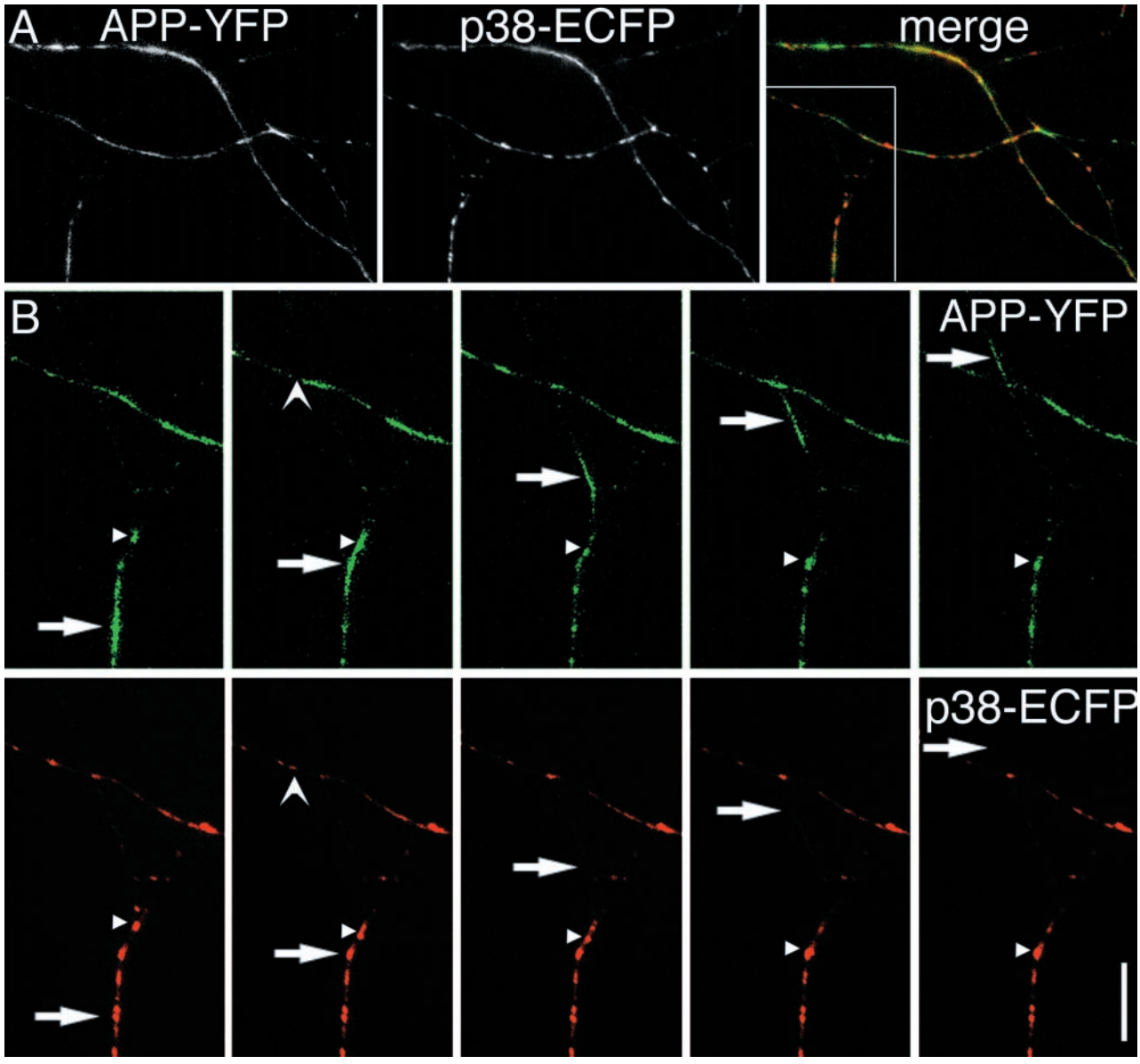

Figure 8. Two-color video microscopy of doubly transfected neurons shows little colocalization of APP-YFP and p38-ECFP (video). Seven- to 8-d-old neurons were doubly transfected with APP-YFP and p38-ECFP cDNA, and two-color video microscopy was performed as described in MATERIALS AND METHODS. (A), Left, frames showing APP-YFP (video); middle, frames showing p38-EGFP (video); right, merged images (video). APP-YFP is shown in green; p38-ECFP is shown in red. (B) Five subsequent frames from the boxed area in A are displayed separately. Top row, APP-YFP; bottom row, p38-ECFP. Arrows mark the position of a fast-moving APP-YFP–positive, p38-ECFP–negative tubule; arrowheads mark the position of a retrogradely moving vesicular structure containing both proteins. The triangle marks the position of a p38-ECFP–positive, APP-YFP–negative structure moving to the right of the image. The total number of frames is 20 pairs, recorded during 64 s. Bar, 10 μm.

proteins is visualized simultaneously. The observed difference in velocities between the two types of carriers in the same neuron is consistent with the idea that the transport is mediated by different motor proteins (Hirokawa, 1998).

Why Is There No Bias in the Transport of p38-EGFP?

In steady state, p38-EGFP is distributed along the axon. Therefore, a net anterograde transport of newly synthesized protein would be expected, which is not observed in our system. Because both endosomes and transport carriers show movement in both directions (Nakata *et al.*, 1998; Prekeris *et al.*, 1999), and because p38-EGFP is present in both types of organelles (Nakata *et al.*, 1998; this study), it is possible that a net anterograde movement of p38-EGFP transport vesicles is masked. Therefore, even a slight net anterograde movement that is not detectable in our system could still account for the distribution of p38-EGFP–labeled

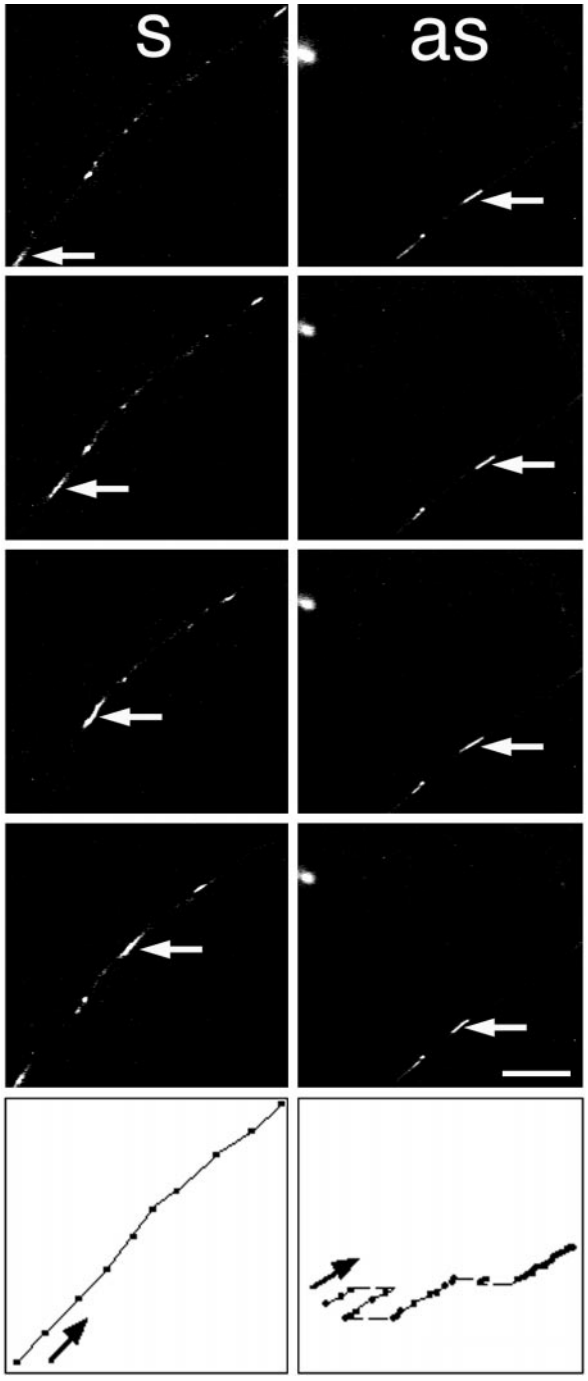

Figure 9. KHC antisense treatment interferes with axonal transport of APP-YFP (video). Seven- to 8-d-old neurons were transfected with APP-YFP and incubated overnight with sense (s) and antisense (as) oligonucleotides corresponding to KHC. Video microscopy was performed, and tracks were analyzed. Every second frame of eight frames and the corresponding track displays are shown for both conditions. Top, anterograde. Total length: sense, 34 frames recorded in 44 s; antisense, 71 frames recorded in 123 s. Bar, 10 μm.

organelles along the axon, because there is sufficient time for equilibration between transfection and microscopy.

What Defines the Structure of the APP-YFP Tubules?

The axon is packed with cytoskeletal elements, transport carriers moving in both directions, mitochondria, and other organelles. Elongation of big vesicles might be a consequence of dragging this vesicle through a dense network. Indeed, mitochondria in axons are also very thin and elongated (Morris and Hollenbeck, 1995). Moreover, we occasionally observed APP-YFP tubules that rounded up shortly after stopping (our unpublished results). APP-YFP–containing carriers could be bigger than those containing p38-EGFP; therefore, they could be more subjected to mechanical stress and be forced into a tubular shape. Alternatively, the two carriers could be of different rigidity because of differences in lipid and protein composition, therefore responding differently to the mechanical forces they encounter when squeezed through the dense axonal cytoplasm. When the GFP fusion proteins were expressed in COS cells, we could detect tubules only in the APP-YFP–transfected cells, not in p38-EGFP–transfected cells (our unpublished results). This suggests that also in unpolarized cells they are sorted into distinct carriers that differ in their composition.

How Is the Velocity Accomplished?

It has been suggested that in axons the size of an organelle determines its velocity, smaller objects moving faster than bigger ones (Vale *et al.*, 1985b). In our case we observed the opposite: long tubules containing APP-YFP moved much faster than the smaller tubulovesicular structures containing p38-EGFP. The fast movement might reflect a joint effort of the molecular motors that are attached to the tubules, leading to a higher velocity, as would be the case for single or few motors only. The fact that many motors are attached to a tubule might also explain why the movement is smooth and continuous over long distances, in contrast to the typical saltatory movement observed for axonal transport.

Reducing kinesin expression disturbs the transport of APP-YFP carriers. Upon reduction of kinesin, a lower velocity as well as a frequent change of direction were observed. Studies using squid axonal vesicles suggested that there are plus end- as well as minus end-directed motor proteins present and that the ratio between the two determines the direction of movement (Muresan *et al.*, 1996). A similar scenario could be envisioned for mammalian neurons: on APP-YFP–containing tubules both plus end- and minus end-directed motors are present; however, kinesin is dominating. This leads to long-distance movement in one direction only. Treatment of neurons with kinesin antisense oligonucleotides would interfere with this ratio, driving it to a more equilibrated state. This would lead to the frequent change of direction observed in antisense treated neurons. It would be interesting to test the effects of the antisense treatment on the transport of p38-EGFP. However, because of the small-distance movement and the low velocities of p38-EGFP–containing structures, no significant effect was measured using our setup (C. Kaether and C.G. Dotti, unpublished results). Faster image acquisition together with higher sensitivity would be needed to study this process.

Implications on APP Processing

Of principal interest in Alzheimer's disease research is to determine the subcellular localization of APP processing and hence the localization of the different secretases. Precise kinetic studies on Aβ production in neurons are lacking. These are complicated by the fact that they are highly polarized: processing in intracellular organelles could take place in the soma, in the dendrites, or in the axon, or processing could take place at the plasma membranes of one or more of these domains. Our studies help provide tools for a detailed analysis of APP processing in neurons: correlation of the transport kinetics using APP-YFP and video microscopy together with pulse–chase labeling to monitor the processing state could help provide information about the subcellular identity of the cleavage compartment in neurons.

ACKNOWLEDGMENTS

We thank B. Hellias for preparing hippocampal cultures, H.-H. Gerdes for kindly providing antiserum D2, B. de Strooper for APP695 cDNA, R. Pepperkok for YFP5 cDNA, and J. Rietdorf for writing the tracking macro. We also thank M. Hannah, M. Kiebler, D. Toomre, F. Ruberti, and E. Piddini for critically reading the manuscript. C.K. is a recipient of a fellowship from the Fritz-Thyssen-Stiftung.

REFERENCES

Allen, R.D., Metuzals, J., Tasaki, I., Brady, S.T., and Gilbert, S.P. (1982). Fast axonal transport in squid giant axon. Science *218*, 1127–1129.

Amaratunga, A., Morin, P.J., Kosik, K.S., and Fine, R.E. (1993). Inhibition of kinesin synthesis and rapid anterograde axonal transport in vivo by an antisense oligonucleotide. J. Biol. Chem. *268*, 17427–17430.

Bloom, G.S., Richards, B.W., Leopold, P.L., Ritchey, D.M., and Brady, S.T. (1993). GTP gamma S inhibits organelle transport along axonal microtubules. J. Cell Biol. *120*, 467–476.

Bradke, F., and Dotti, C.G. (1997). Neuronal polarity: vectorial cytoplasmic flow precedes axon formation. Neuron *19*, 1175–1186.

Brady, S.T. (1985). A novel brain ATPase with properties expected for the fast axonal transport motor. Nature *317*, 73–75.

Brady, S.T., Pfister, K.K., and Bloom, G.S. (1990). A monoclonal antibody against kinesin inhibits both anterograde and retrograde fast axonal transport in squid axoplasm. Proc. Natl. Acad. Sci. USA *87*, 1061–1065.

Bridgman, P.C. (1999). Myosin Va movements in normal and dilute-lethal axons provide support for a dual filament motor complex. J. Cell Biol. *146*, 1045–1060.

Buxbaum, J.D., Thinakaran, G., Koliatsos, V., O'Callahan, J., Slunt, H.H., Price, D.L., and Sisodia, S.S. (1998). Alzheimer amyloid protein precursor in the rat hippocampus: transport and processing through the perforant path. J. Neurosci. *18*, 9629–9637.

Craig, A.M., and Banker, G. (1994). Neuronal polarity. Annu. Rev. Neurosci. *17*, 267–310.

de Hoop, M.J., Meyn, L., and Dotti, C.G. (1998). Culturing hippocampal neurons and astrocytes from fetal rodent brain. In: Cell Biology: A Laboratory Handbook, ed. J.E. Celis, San Diego: Academic Press, 154–163.

Dotti, C.G., Sullivan, C.A., and Banker, G.A. (1988). The establishment of polarity by hippocampal neurons in culture. J. Neurosci. *8*, 1454–1468.

Ellenberg, J., Lippincott, S.J., and Presley, J.F. (1999). Dual-color imaging with GFP variants. Trends Cell Biol. *9*, 52–56.

Ferreira, A., Caceres, A., and Kosik, K.S. (1993). Intraneuronal compartments of the amyloid precursor protein. J. Neurosci. *13*, 3112–3123.

Ferreira, A., Niclas, J., Vale, R.D., Banker, G., and Kosik, K.S. (1992). Suppression of kinesin expression in cultured hippocampal neurons using antisense oligonucleotides. J. Cell Biol. *117*, 595–606.

Hardy, J. (1997). Amyloid, the presenilins and Alzheimer's disease. Trends Neurosci. *20*, 154–159.

Hirokawa, N. (1997). The mechanisms of fast and slow transport in neurons: identification and characterization of the new kinesin superfamily motors. Curr. Opin. Neurobiol. *7*, 605–614.

Hirokawa, N. (1998). Kinesin and dynein superfamily proteins and the mechanism of organelle transport. Science *279*, 519–526.

Hirokawa, N., Noda, Y., and Okada, Y. (1998). Kinesin and dynein superfamily proteins in organelle transport and cell division. Curr. Opin. Cell Biol. *10*, 60–73.

Hirschberg, K., Miller, C.M., Ellenberg, J., Presley, J.F., Siggia, E.D., Phair, R.D., and Lippincott, S.J. (1998). Kinetic analysis of secretory protein traffic and characterization of Golgi to plasma membrane transport intermediates in living cells. J. Cell Biol. *143*, 1485–1503.

Köhrmann, M., Luo, M., Kaether, C., DesGroseillers, L., Dotti, C.G., and Kiebler, M.A. (1999). Microtubule-dependent recruitment of Staufen-green fluorescent protein into large RNA-containing granules and subsequent dendritic transport in living hippocampal neurons. Mol. Biol. Cell *10*, 2945–2953.

Koo, E.H., Sisodia, S.S., Archer, D.R., Martin, L.J., Weidemann, A., Beyreuther, K., Fischer, P., Masters, C.L., and Price, D.L. (1990). Precursor of amyloid protein in Alzheimer disease undergoes fast anterograde axonal transport. Proc. Natl. Acad. Sci. USA *87*, 1561–1565.

Kreis, T.E., Matteoni, R., Hollinshead, M., and Tooze, J. (1989). Secretory granules and endosomes show saltatory movement biased to the anterograde and retrograde directions, respectively, along microtubules in AtT20 cells. Eur. J. Cell Biol. *49*, 128–139.

Leube, R.E., *et al*. (1987). Synaptophysin: molecular organization and mRNA expression as determined from cloned cDNA. EMBO J. *6*, 3261–3268.

Lochner, J.E., Kingma, M., Kuhn, S., Meliza, C.D., Cutler, B., and Scalettar, B.A. (1998). Real-time imaging of the axonal transport of granules containing a tissue plasminogen activator/green fluorescent protein hybrid. Mol. Biol. Cell *9*, 2463–2476.

Morris, R.L., and Hollenbeck, P.J. (1995). Axonal transport of mitochondria along microtubules and F-actin in living vertebrate neurons. J. Cell Biol. *131*, 1315–1326.

Muresan, V., Godek, C.P., Reese, T.S., and Schnapp, B.J. (1996). Plus-end motors override minus-end motors during transport of squid axon vesicles on microtubules. J. Cell Biol. *135*, 383–397.

Nakata, T., Terada, S., and Hirokawa, N. (1998). Visualization of the dynamics of synaptic vesicle and plasma membrane proteins in living axons. J. Cell Biol. *140*, 659–674.

Noda, Y., Sato, Y.R., Kondo, S., Nangaku, M., and Hirokawa, N. (1995). KIF2 is a new microtubule-based anterograde motor that transports membranous organelles distinct from those carried by kinesin heavy chain or KIF3A/B. J. Cell Biol. *129*, 157–167.

Ochs, S. (1972). Fast transport of materials in mammalian nerve fibers. Science *176*, 252–260.

Okada, Y., Yamazaki, H., Sekine, A.Y., and Hirokawa, N. (1995). The neuron-specific kinesin superfamily protein KIF1A is a unique mo-

nomeric motor for anterograde axonal transport of synaptic vesicle precursors. Cell *81*, 769–780.

Pepperkok, R., Squire, A., Geley, S., and Bastiaens, P.I. (1999). Simultaneous detection of multiple green fluorescent proteins in live cells by fluorescence lifetime imaging microscopy. Curr. Biol. *9*, 269–272.

Prekeris, R., Foletti, D.L., and Scheller, R.H. (1999). Dynamics of tubulovesicular recycling endosomes in hippocampal neurons. J. Neurosci. *19*, 10324–10337.

Selkoe, D.J. (1999). Translating cell biology into therapeutic advances in Alzheimer's disease. Nature *399*, A23–A31.

Simons, M., Ikonen, E., Tienari, P.J., Cid, A.A., Monning, U., Beyreuther, K., and Dotti, C.G. (1995). Intracellular routing of human amyloid protein precursor: axonal delivery followed by transport to the dendrites. J. Neurosci. Res. *41*, 121–128.

Storey, E., Katz, M., Brickman, Y., Beyreuther, K., and Masters, C.L. (1999). Amyloid precursor protein of Alzheimer's disease: evidence for a stable, full-length, trans-membrane pool in primary neuronal cultures. Eur. J. Neurosci. *11*, 1779–1788.

Stowell, J.N., and Craig, A.M. (1999). Axon/dendrite targeting of metabotropic glutamate receptors by their cytoplasmic carboxy-terminal domains (see comments). Neuron *22*, 525–536.

Toomre, D., Keller, P., White, J., Olivo, J.C., and Simons, K. (1999). Dual-color visualization of trans-Golgi network to plasma membrane traffic along microtubules in living cells. J. Cell Sci. *112*, 21–33.

Vale, R.D., Reese, T.S., and Sheetz, M.P. (1985a). Identification of a novel force-generating protein, kinesin, involved in microtubule-based motility. Cell *42*, 39–50.

Vale, R.D., Schnapp, B.J., Reese, T.S., and Sheetz, M.P. (1985b). Movement of organelles along filaments dissociated from the axoplasm of the squid giant axon. Cell *40*, 449–454.

Wacker, I., Kaether, C., Krömer, A., Migala, A., Almers, W., and Gerdes, H.-H. (1997). Microtubule-dependent transport of secretory vesicles visualized in real time with a GFP-tagged secretory protein. J. Cell Sci. *110*, 1453–1463.

Weidemann, A., Konig, G., Bunke, D., Fischer, P., Salbaum, J.M., Masters, C.L., and Beyreuther, K. (1989). Identification, biogenesis, and localization of precursors of Alzheimer's disease A4 amyloid protein. Cell *57*, 115–126.

Wessel, D., and Flügge, U.I. (1984). A method for quantitative recovery of protein in dilute solution in the presence of detergent and lipids. Anal. Biochem. *138*, 141–143.

Winckler, B., and Mellman, I. (1999). Neuronal polarity: controlling the sorting and diffusion of membrane components (in process citation). Neuron *23*, 637–640.

Yamazaki, T., Selkoe, D., and Koo, E.H. (1995). Trafficking of cell surface β-amyloid precursor protein: retrograde and transcytotic transport in cultured neurons. J. Cell Biol. *129*, 431–442.

Yonekawa, Y., Harada, A., Okada, Y., Funakoshi, T., Kanai, Y., Takei, Y., Terada, S., Noda, T., and Hirokawa, N. (1998). Defect in synaptic vesicle precursor transport and neuronal cell death in KIF1A motor protein-deficient mice. J. Cell Biol. *141*, 431–441.

Zakharenko, S., and Popov, S. (1998). Dynamics of axonal microtubules regulate the topology of new membrane insertion into the growing neurites. J. Cell Biol. *143*, 1077–1086.